Journal of Controlled Release 340 (2021) 209–220

Contents lists available at ScienceDirect

Journal of Controlled Release

journal homepage: www.elsevier.com/locate/jconrel

# A respirable HPV-L2 dry-powder vaccine with GLA as amphiphilic lubricant and immune-adjuvant

Irene Rossi [a,c,1,2], Gloria Spagnoli [b,c,1], Francesca Buttini [a,c], Fabio Sonvico [a,c], Fabio Stellari [d], Davide Cavazzini [b], Quigxin Chen [e], Martin Müller [e], Angelo Bolchi [b,c], Simone Ottonello [b,c,*], Ruggero Bettini [a,c,*]

[a] Department of Food and Drug Sciences, University of Parma, Parco Area delle Scienze Parma, Italy
[b] Department of Chemistry, Life Sciences and Environmental Sustainability, University of Parma, Parco Area delle Scienze Parma, Italy
[c] Interdepartmental Center Biopharmanet-tec, University of Parma, Parco Area delle Scienze Parma, Italy
[d] Chiesi Farmaceutici SpA, Largo Belloli 11a, Parma, Italy
[e] German Cancer Research Center, Im Neuenheimer Feld 280, Heidelberg, Germany

ARTICLE INFO

*Keywords:*
Pulmonary vaccination
Dry powder for inhalation
Spray drying
Human papillomavirus
Glucopyranosyl lipid A

ABSTRACT

Vaccines not requiring cold-chain storage/distribution and suitable for needle-free delivery are urgently needed. Pulmonary administration is one of the most promising non-parenteral routes for vaccine delivery. Through a multi-component excipient and spray-drying approach, we engineered highly respirable dry-powder vaccine particles containing a three-fold repeated peptide epitope derived from human papillomavirus (HPV16) minor capsid protein L2 displayed on *Pyrococcus furious* thioredoxin as antigen. A key feature of our engineering approach was the use of the amphiphilic endotoxin derivative glucopyranosyl lipid A (GLA) as both a coating agent enhancing particle de-aggregation and respirability as well as a built-in immune-adjuvant. Following an extensive characterization of the *in vitro* aerodynamic performance, lung deposition was verified *in vivo* by intratracheal administration in mice of a vaccine powder containing a fluorescently labeled derivative of the antigen. This was followed by a short-term immunization study that highlighted the ability of the GLA-adjuvanted vaccine powder to induce an anti-L2 systemic immune response comparable to (or even better than) that of the subcutaneously administered liquid-form vaccine. Despite the very short-term immunization conditions employed for this preliminary vaccination experiment, the intratracheally administered dry-powder, but not the subcutaneously injected liquid-state, vaccine induced consistent HPV neutralizing responses. Overall, the present data provide proof-of-concept validation of a new formulation design to produce a dry-powder vaccine that may be easily transferred to other antigens.

## 1. Introduction

Vaccination is an established cost-effective strategy for the prevention of infectious (and some non-infectious) diseases [1,2] and its value as a life-saving tool is all the more appreciated during the present SARS-CoV2 pandemics [3]. Regardless of their attenuated/inactivated whole virus or recombinant nature, most present-day vaccines require a strict cold-chain maintenance to remain active. Indeed, cold-chain maintenance accounts for approximately 50% of vaccine cost on average and a similar fraction of the total vaccine production is thought to be wasted or damaged due to cold-chain breakage [4,5]. This is both an economical and a healthcare problem, which especially (but not exclusively)

*Abbreviations:* GLA, Glucopyranosyl Lipid A; MPLA, Monophosphoryl Lipid A; HPV16, Human Papillomavirus; S.C., Subcutaneous; I.T., Intratracheal; DPI, Dry Powder Inhaler; EM, Emitted Mass; EF, Emitted Fraction; RM, Respirable Mass; RF, Respirable Fraction; MMAD, Mass Median Aerodynamic Diameter; GSD, Geometrical Standard Deviation; FSI, Fast Screening Impactor; ACI, Andersen Cascade Impactor; PSD, Particle Size Distribution; SEM, Scanning Electron Microscopy; DVS, Dynamic Vapor Sorption; TGA, Thermogavimetric Analysis; ELISA, Enzyme-Linked Immunosorbent Assay; SDS-PAGE, Sodium Dodecyl Sulphate Polyacrylamide Gel Electrophoresis; Micro-CT, Micro-Computed Tomography; IVIS, *In vivo* Imaging System.

* Corresponding authors at: Parco Area delle Scienze 27/A, 43124 Parma, Italy.
*E-mail addresses:* simone.ottomnello@unipr.it (S. Ottonello), ruggero.bettini@unipr.it (R. Bettini).

[1] Equally contributing to the paper.
[2] Present address: Nanopharm Ltd., An Aptar Pharma Company, Newport, United Kingdom.

https://doi.org/10.1016/j.jconrel.2021.11.002
Received 4 June 2021; Received in revised form 16 September 2021; Accepted 1 November 2021
Available online 3 November 2021

impacts on low-and-middle-income countries (LMICs), that is the very places where vaccination is most needed. An additional drawback associated to most current vaccines is that they are commonly administered *via* intramuscular (i.m.) or subcutaneous (s.c.) injection. This mode of delivery requires trained medical personnel, may face religious and/or ethnical barriers, and comes with the inherent risk, especially in LMICs, of needle-stick related injuries and potential infections. Even in high-income countries, adverse reactions to parenteral, needle-requiring vaccine administration (so-called 'lipothymic reaction' or 'needle-phobia') [6] as well as the burden of this mode of administration on the healthcare system have been documented.

Novel vaccine formulations, compatible with viral and protein-based subunit antigens, suitable for non-parenteral administration are thus actively sought as a possible solution to the above-described limitations. Solid-dosage vaccines (*i.e.*, lyophilized or powder form vaccines) are reportedly more stable than their corresponding liquid forms, both from the biochemical (*i.e.*, antigen structural integrity) and microbiological point of view, due to the absence of water [7]. This makes them amenable to non-cold-chain distribution and a more effective stock-piling. However, due to the general sensitivity of proteins to dehydration, water removal is a risky step for the maintenance of antigen integrity. These potentially adverse effects can be supressed, or at least minimized, by the addition of sugars (*e.g.* trehalose), polyols (*e.g.* mannitol), polysaccharides (*e.g.* dextran) or amino acids (*e.g.* L-leucine) as stabilizing agents and antigen-protective excipients [8–14].

Among the various routes of non-parenteral vaccine administration, pulmonary vaccination is gaining momentum due to several favorable features. These include the large surface area, extended vascularization and abundance of dendritic cells and macrophages for antigen capture of the respiratory tract, without exposure to a harsh environment such as the one found in the gastro-intestinal tract. This, coupled with direct antigen delivery to a mucosal site, may result in a more effective mucosal immunity without any interference with systemic immunity, thus allowing for a broad application of this mode of immunization. An additional advantage of pulmonary vaccination is its needle-free administration -a mode of delivery that in humans is facilitated by the availability of well-developed dry powder inhalers [14].

The first attempts at pulmonary vaccination date back to the late 60's. These were based on the inhalatory administration of either very low amounts of living attenuated *Mycobacterium bovis* [15] or a liquid-form of aerosolized influenza vaccine [16], both of which led to successful immunization and protection. Despite these promising initial results, follow-up studies on pulmonary vaccination were discontinued, likely due to the lack of easy-to-use administration devices. They were resumed more than 35 years later and extended to non-airborne infections such as hepatitis B (HBV), diphtheria and measles (see #7 for a review). HBV and influenza have been the predominant test-bench of pulmonary vaccination, and different types of variously adjuvanted immunogens, relying on inactivated whole-virus but also on recombinant antigens, formulated by spray-freeze-drying and delivered in either a liquid or a powder form have been investigated in different preclinical settings for their lung deposition and immunogenicity [7,17,18].

In addition to the specific types of antigen and immune-adjuvant, the physical state of the vaccine as well as its formulation and manufacturing, have also been shown to strongly influence the immune performance of inhalatory vaccines [10,17,19–22]. Of note, powder vaccine formulations have generally been found to be comparable, or superior, to liquid antigen formulations with regard to immunogenicity, but with the added benefits of long-term stability and ease of delivery [7,10,17,18,20–22]. Particle size and shape, and particularly an aerodynamic diameter smaller than 5 μm, are key features for achieving a suitable lung deposition [17–19]. Among the different drying processes used to produce respirable particles, spray-drying stands up as the most easily scalable procedure. Also, the aerodynamic performance of spray-dried powders has been shown to be significantly improved by a particle engineering approach involving the addition of small amounts of surfactant or amphiphilic molecules with lubricant functionality [23,24].

Similar to most presently licensed vaccines, current human papillomavirus (HPV) vaccines, which rely on different combinations of major capsid protein L1 virus-like particles (VLP) [25], also have to be continuously refrigerated during storage/distribution [26]. Following-up to the encouraging results obtained with liquid-state, monotypic (HPV16) VLPs delivered through the airways *via* nasal nebulization or bronchial aerosolization [27], two different dry-powder HPV vaccine formulations were developed and tested for thermal stability and immunogenicity upon i.m. injection [28–30]. These powder vaccine formulations were produced by either a multicomponent excipient, spray-dry system [28,29], or with the use of glass forming polymers and trehalose as spray-drying excipients followed by atomic layer deposition to coat the resulting particles with defined layers of the alum adjuvant [30]. Except for one study dealing with the thermal stability of a spray-dried formulation of the nonavalent Gardasil® 9 HPV vaccine [28], the other studies were focused on simplified, intrinsically more thermostable HPV antigens such as L1 capsomeres [30] and a peptide epitope from minor capsid protein L2 incorporated into MS2 bacteriophage VLPs [29]. A substantial increase in thermal stability along with an immunogenicity comparable to, or even higher than, that of liquid vaccine controls was observed for both spray-dried and alum-coated vaccine formulations. However, the resulting vaccine powders were always dissolved prior to immunization, which was only performed by intramuscular injection, thus obviously precluding any information on dry-powder vaccine respirability, lung deposition and immunogenicity upon pulmonary delivery.

To begin to fill these gaps, we developed and tested a dry-powder inhalatory (DPI) formulation of a HPV vaccine based on a previously described L2 antigen [31,32], in which three copies of the HPV16 L2 major cross-neutralization epitope comprised between amino acids 20–38 are grafted intramolecularly to *Pyrococcus furiosus* thioredoxin (hereafter designated as *Pf*Trx-HPV-L2). The thermal stability and immunogenicity of this particular antigen [31,32] as well as the pre-clinical efficacy and cross-neutralization capacity of other antigens based on a similar L2 epitope [33] have been documented previously.

The *Pf*Trx-HPV-L2 DPI vaccine was produced by spray-drying through a particle engineering approach based on the molecular deposition of an amphiphilic immune-adjuvant (glucopyranosyl lipid A; GLA) on the surface of the spray-dried particles. The rationale behind this approach was to improve both particle respirability as well as surface exposure of the adjuvant and its recognition by lung immune cells, especially antigen presenting cells such as dendritic cells and macrophages [18]. The dry powder vaccine thus produced was extensively characterized with respect to aerodynamic properties, including the assessment of its *in vivo* lung deposition capacity. The systemic immunogenicity of the intratracheally delivered *Pf*Trx-HPV-L2 DPI vaccine was also preliminarily evaluated in a short-term immunization study in mice.

## 2. Materials and methods

### 2.1. Materials

Mannitol, Pearlitol® SD 200 batch no. E556G, was a kind gift by Roquette Freres. Sodium stearate was purchased from Magnesia GmbH. Glycopyranoside Lipid A (GLA, pHAD), a synthetic version of Monophosphoryl Lipid A (MPLA), was supplied by Avanti Polar Lipids. All solvents were of analytical grade and ultrapure water (0.055 μS/cm, TOC 1 ppb) was produced by reverse osmosis (Purelab Pulse + Flex ultrapure water, Elga-Veolia).

## 2.2. Methods

### 2.2.1. PfTrx-HPV-L2 and GST-L2 constructs

Codonusage-optimized *Pyrococcus furiosus* (*Pf*) Trx (*Pf*Trx) coding sequences were chemically synthesized (Eurofins MWG Operon) and inserted into the *NdeI* site of a His-tag-lacking pET26 plasmid. Three tandemly repeated copies of the HPV16 L2 aa 20-38 peptide grafted into the display site of *Pf*Trx was generated by inserting the corresponding sequences into the Trx *CpoI* sites of pre-assembled pET-*Pf*Trx plasmids as described previously [31,32,34]. The resulting constructs were sequence-verified and transformed into *Escherichia coli* BL21 codon plus (DE3) cells for recombinant protein expression.

Glutathione S-transferase (GST)-L2 fusion to be used as capture antigen for ELISA was produced by cloning the L2 (aa 1–120) coding sequence into the *SmaI* site of the GST expression vector pGEX-4 T-2.

### 2.2.2. Expression and purification of the PfTrx-HPV-L2 antigen

Recombinant *Pf*Trx-HPV-L2 was produced by overnight induction at 30 °C in auto-inducer medium (10 g/L yeast extract, 25 mM $NH_4SO_4$, 50 mM $KH_2PO_4$, 50 mM $Na_2HPO_4$, 2 mM glucose, 6 mM α-lactose, 1.2 mM $MgSO_4$). Following cell lysis, the untagged *Pf*Trx-HPV-L2 protein was purified by cation exchange chromatography and detoxified by a three-fold repeated Triton X-114 (1% *v*/v) treatment [35]. Endotoxin (LPS) removal, to levels lower than 2 EU/mL, was verified for each antigen batch by the LAL QLC-1000 test (Lonza). The GST-L2 protein was affinity-purified on Glutathione-Sepharose columns (GE Healthcare) according to the manufacturer's instructions. The composition and purity of individual protein preparations were assessed by electrophoretic analysis on 11–15% SDS-polyacrylamide gels (SDS-PAGE). Protein concentration was determined by measurement of absorbance at 280 nm using calculated extinction coefficients [36] and with the use of a QubitH 2.0 Fluorometer (Life Technologies).

### 2.2.3. Spray-drying

Dried engineered powders for inhalation containing the antigen were produced by spray-drying with a mini Spray Dryer Büchi B-290 (Büchi Laboratoriums-Technik) in aspiration and open mode. The feed solution was prepared by dissolving the bulking agent in ultrapure water, whereas the amphiphilic compound was dissolved in ethanol (95% *v*/v). The protein solution in 25 mM potassium phosphate buffer (pH 7.4) was then added to the water portion and the ethanol solution was added drop-wise to the aqueous solution under continuous magnetic stirring at 200 rpm to reach a final solution with a water to ethanol ratio of 70:30 *v/v*. The total concentration of solutes was always kept at 0.6% *w/v*.

The concentration of the bulking agent in the solution was adjusted for each formulation to complement 0.6% *w/v* of the total solute taking into consideration the concentrations of the protein and of the amphiphilic compound. Formulations of the main powder tested are summarized in Table S1 (Supplementary). The drying parameters were set as follows: inlet temperature, 125 °C; drying air flow rate, 601 L/h; aspiration, 35 $m^3$/h; solution feed rate, 3.5 mL/min and nozzle diameter, 0.7 mm.

### 2.2.4. Particle size distribution by laser diffraction

The particle size distribution (PSD) of spray-dried powders was measured by laser light scattering (Spraytec®, Malvern Instruments Ltd). The diffractometer was equipped with a 300 mm focal lens, which measures particle sizes in the range 0.1–900 μm. Samples were prepared by suspending 10 mg of individual powders in 10 mL of cyclohexane containing 0.1% *w/v* of Span 85 (Honeywell Fluka™). To improve homogeneity, the dispersion was put in an ultrasonic bath (8510, Branson Ultrasonics Corporation) for 5 min before PSD measurements that were carried out in triplicate for each sample with an obscuration threshold of at least 10%. Data are expressed as volume diameter of 10th ($D_{v,10}$), 50th ($D_{v,50}$) and 90th ($D_{v,90}$) percentile of the particle population and as Span value [$(D_{v,90}$-$D_{v,10})/D_{v,50}$].

### 2.2.5. Scanning electron microscopy and powder flow

A Scanning Electron Microscope (FESEM-FIB Zeiss Auriga Compact, Carl Zeiss) was used to investigate particle morphology, shape and surface characteristics of the spray-dried powders. Powders were deposited onto adhesive black carbon tabs pre-mounted on aluminum stubs; powder in excess was removed with a gentle nitrogen flow and samples imaged without any metallization. The microscope was operated after 30 min of depressurization ($1.87\ 10^{-4}$ Pa) with an accelerating voltage of 1.0 kV and a working distance of 4.9 mm. Images were taken at different magnifications.

Dynamic angle of repose was determined as an indicator of the powder flow properties. Measurements were carried out according to Ph. Eur. (10th ed.) employing a Friability tester (model TA3R, Erweka GmbH) where the drum had been removed and replaced with a transparent glass vial (volume 10 mL) filled with about 50 mg of powder. The vial was then attached to the tester arm and rotated for 60 s at 20 rpm. A video was recorded with an iPhone 6 (Apple) and single frames were extracted and analyzed with the software Image J64 (NIH) to measure the angle between the horizontal lane and the powder avalanche line during the so-called rolling stage. Six independent measurements were performed for each tested powder.

### 2.2.6. In vitro aerodynamic performance assessment

The aerodynamic performance of the powders was firstly investigated using a Fast Screening Impactor(FSI; Copley Scientific Ltd). 10 mg of powder were loaded manually in a hypromellose Quali-V-I capsule size 3 (Qualicaps) and one single capsule for each test was aerosolized using a high-resistance RS01® device (RPC, Plastiape). The entire system was connected to a vacuum pump (Erweka GmbH, Mod. 1000), which created the air flow to aerosolize and distribute the powder in the FSI. The flow rate used during each test was adjusted according to a current USP monograph, with a Critical Flow Controller TPK (Copley Scientific Ltd) in order to produce a pressure drop of 4 kPa over the inhaler. Thus, flow rate was set at 60 L/min before each experiment using a Flow Meter DFM 2000 (Copley Scientific Ltd). The pump was activated for 4 s in each test, so to withdraw a volume of 4 L of air from the inhaler. The aerosolization performance was tested in triplicate. The following parameters were calculated: the emitted mass (EM) was the amount of powder emitted from the device; the emitted fraction (EF) was calculated as the ratio between the EM and the amount of powder loaded into the capsule. The respirable mass (RM) was the mass of powder with an aerodynamic diameter lower than 5 μm, *i.e.*, the amount deposited on the filter (type A/E, 76 mm diameter 76, Pall Corporation) of the Fine Fraction Collector (FFC); the respirable mass (RF) was calculated as the ratio between RM and the amount of powder loaded into the capsule. EM and RM were calculated from the weight of the device loaded with the filled capsule and the filter before and after aerosolization of the powder.

Andersen Cascade Impactor (ACI, Apparatus 3, USP 41, Copley scientific Ltd) was employed to determine the aerodynamic distribution of the powder produced for the *in vivo* study. The measurements were carried out according to USP-NF <601> thus, at the flow rate of 60 L/min (see below), the cut-off diameters of stages −1, −0, 1, 2, 3, 4, 5 and 6 were the following: 8.60, 6.50, 4.40, 3.20, 1.90, 1.20, 0.55 and 0.26 μm. A glass microfiber filter of diameter 82.6 mm (Whatman plc) was placed right below stage six to collect particles with a diameter smaller than that 0.26 μm. 20 mg of each powder were loaded into Quali-V-I size 3 capsules and the RS01® device was again employed for the aerosolization. Before running the experiment, 2 mL of a solution of Tween® 1% *w/v* in ethanol was applied to the particle collection surface of each stage; after complete solvent evaporation, a thin layer of surfactant was obtained on the stage surfaces that ensured efficient particle capture avoiding particle bouncing. An air flow rate of set at 60 L/min, (Flow Meter DFM 2000) was generated by a vacuum pump (SCP5, Copley scientific Ltd) activated for 4 s, using the TPK to adjust the flow. After powder aerosolization, the powder deposited in the device was

cumulated with the residual powder in the capsule and collected with ultrapure water in a 50 mL volumetric flask; a similar collection procedure was followed for the powder deposited in the induction port. The powders deposited onto stages −1, −0 and 1 were solubilized individually with 25 mL of ultrapure water, while 10 mL were used for all the other stages. The filter was removed from the system, put in a crystallizer with 10 mL of ultrapure water and placed for 5 min in an ultrasonic bath. The solutions obtained from the filter as well as from the device plus capsule were filtered through a 0.45 μm cellulose acetate syringe filter (Labservice Analytica) before injection into the HPLC for the quantification of mannitol that was taken as tracer of the particles. Starting at the final collection site (filter), the cumulative mass *versus* cut-off diameter of the respective stage was derived. The mass of mannitol with an aerodynamic diameter less than 5 μm (Fine Particle Dose or Respirable Mass, RM) was calculated by interpolation. Several different aerodynamic parameters were also calculated: Emitted Mass (EM), the mannitol mass collected from the induction port to the filter; Emitted Fraction (EF), the % ratio between the EM and the amount of powder loaded in the capsule; Respirable Fraction (RF), percentage of the RM with respect to the EM. Moreover, the Mass Median Aerodynamic Diameter (MMAD) defined as the diameter which separates the powder in two populations of equal weight was determined by plotting the cumulative percentage of mass less than the cut-off diameter for each stage on a probability scale *versus* the relevant aerodynamic diameter of the stage on a logarithmic scale. MMAD is the slope of the line obtained by linear regression of the experimental points. Finally, the Geometrical Standard Deviation (GSD), a parameter indicating the wideness of the particle size distribution, was calculated as the square root of the ratio between the size of the 84.13% of the particle population in the log-normal distribution and the size of the 15.87% of the particle population in the log-normal distribution.

#### 2.2.7. Mannitol HPLC analysis

A Shimadzu VP (Shimadzu Corporation) high performance liquid chromatographic (HPLC) system coupled with refractive index detector (RID-10A, Shimadzu) set at 40 °C was used for mannitol quantification, following the analytical method reported in the relevant monography by the United States Pharmacopeia (USP 41). Ultrapure water was employed as mobile phase at a flow rate of 1 mL/min with an injection volume set at 100 μL on a Waters 717 plus autosampler (Waters Corporation). An Aminex® HPX-87H Ion Exclusion, 300 mm × 7.8 mm (Bio-Rad, Hercules) column was used as stationary phase. The column was equilibrated at 80 °C for 2 h with the mobile phase pumped at 0.2 mL/min and maintained at that temperature during the chromatographic runs. A Shimadzu Class VP software was used for data acquisition and analysis. Each sample was injected six times and the three closer values were used to calculate the mean and standard deviation. Linearity of the responses was assessed between 0.01 mg/mL and 1 mg/mL ($R^2 = 0.999$). The limit of detection and the limit of quantification were 2.6 μg/mL and 8 μg/mL, respectively.

#### 2.2.8. Fluorescent labelling of PfTrx-HPV-L2

The *Pf*Trx-HPV-L2 protein was dissolved in 0.1 M sodium bicarbonate buffer, mixed with the reactive dye solution (Alexa Fluor 750; Life Technologies) and incubated for 1 h at RT with continuous stirring according to the manufacturer's instructions. Separation of the labeled protein from the unreacted free dye was performed by size fractionation (Econo-Pac 10DG Desalting columns, Bio-Rad). Labelling stoichiometry was determined by comparing the absorbance at 280 nm of equally concentrated solutions of the unlabeled and the Alexa-labeled protein. The Alexa-conjugated *Pf*Trx-HPV-L2 antigen incorporated into the DPI at 2% *w/w* of the resulting product, was administered intratracheally to female BALB/c mice in either a PBS pre-dissolved liquid form or in powder form.

#### 2.2.9. Animal experimentation

Female inbred BALB/c mice (7-8 weeks-old) were purchased from Envigo Laboratories (Italy). Prior to use, animals were acclimatized for at least 5 days to the local vivarium conditions (room temperature: 20–24 °C; relative humidity: 40–70%; 12-h light–dark cycle), with free access to standard rodent chow and softened tap water. All animal experiments were approved by the intramural animal welfare committee for animal experimentation (authorization n. 31/2015-PR to Chiesi Farmaceutici for imaging experiments; authorization n. 985/2019-PR to University of Parma for immunization experiments) to comply with the European Directive 2010/63 UE, Italian D. Lgs 26/2014 and the revised "Guide for the Care and Use of Laboratory Animals" (Natl. Res. Council, US Committee, 8th Ed., 2011).

For intratracheal administration, animals were lightly anesthetized with either 2.5% isoflurane delivered in a transparent plastic box or ketamine/xylazine (80 and 10 mg/kg, respectively, administered intraperitoneally) and positioned on the intubation platform, hanging by their incisors placed on the wire. Using a small laryngoscope to visualize the trachea, the Alexa-conjugated *Pf*Trx-HPV-L2 vaccine was intratracheally administered by either a syringe-operated micro-cannula (liquid-form vaccine) or with the use of a modified Penn-Century Dry Powder Insufflator™ (Model DP-4 M) device (dry-powder vaccine) [37].

#### 2.2.10. In vivo and ex-vivo imaging

Three different experimental approaches were utilized for *in vivo* imaging. For fluorescence molecular tomography (FMT 2500; PerkinElmer), the anesthetized animals were carefully positioned in the imaging cassette, which was then placed into the FMT imaging chamber. A near infrared (NIR) laser diode transilluminated the thorax region (*i.e.*, passed light through the body of the animal to be collected on the opposite side) and the resulting signal was detected with a thermoelectrically cooled charge-coupled device camera placed on the opposite side of the imaged animal. Appropriate optical filters allowed the collection of both fluorescence and excitation data sets, and the multiple source-detector fluorescence projections were normalized to the paired collection of laser excitation data. Cumulative fluorescence data were reconstructed using the FMT 2500 system with TrueQuant software version 2.2 (Perkin Elmer) in order to obtain a three-dimensional fluorescence signal quantification within the lungs.

The same animals were analyzed by Micro-Computed Tomography (Micro-CT) imaging, performed 15 min after administration with the use of a Quantum GX Micro CT apparatus (Perkin Elmer) as well as by IVIS Lumina II imaging (Perkin Elmer). Micro-CT images were acquired with an intrinsic retrospective two-phase respiratory gating technique using the following parameters: 90 KV, 88 μA over a total angle of 360° for a total scan time of 4 min.

After *in vivo* imaging, mice were euthanized by anesthetic overdosing, followed by bleeding from the abdominal aorta and organ explantation. *Ex-vivo* imaging was then performed on the lungs, trachea, liver, spleen, and kidneys by IVIS Lumina II.

Portions of the explanted lungs, trachea and liver (5 mg of frozen tissue each) were suspended in 300 μL of RIPA buffer [50 mM Tris-HCl, 150 mM NaCl, 1.0% (*v*/v) NP-40, 0.5% (*w/v*) Sodium Deoxycholate, 0.1% (w/v) SDS, pH 8.0], disrupted by sonication (Misonix Sonicator 3000; 20 min, 20% power) and, after centrifugation for 20 min at 10000 x*g*, the resulting supernatants were fractionated by SDS-PAGE, followed by detection of the Alexa-labeled *Pf*Trx-HPV-L2 protein by near-infrared fluorescence at 800 nm, using a ChemiDoc MP Imaging System (Bio-Rad).

#### 2.2.11. Animal immunization

Mice were subdivided into four groups (three controls and one test group), which were injected subcutaneously (s.c.) with three doses (1 priming and 2 boosts) of a solubilized control powder (#1), liquid antigen (#2), solubilized vaccine powder (#3) or the same powder administered intratracheally (#4) at weekly intervals. Group #1 was

comprised of five animals, which were s.c. injected with 1 mg of GLA-containing but antigen-lacking powder dissolved in 50 μL of PBS right before administration. Group #2, comprised of 7 animals, was s.c. injected with the detoxified and filter-sterilized liquid *Pf*Trx-HPV-L2 antigen (20 μg) adjuvanted with 50 μg of aluminum hydroxide (Brenntag) and 10 μg of GLA. Group #3, also comprised of seven animals, was s.c. injected with 1 mg of GLA-containing, *Pf*Trx-HPV-L2 vaccine powder, solubilized in 50 μL of PBS right before administration Test group #4 was comprised of ten mice, to which the GLA-containing, *Pf*Trx-HPV-L2-vaccine powder (~2 mg) was administered intratracheally with the use of a modified Dry Powder Insufflator™ device as described above. The average amount of vaccine powder emitted from the insufflator was pre-determined by weighting the device before and after insufflation. As revealed by these measurements, approximately 50% of the loaded powder was emitted from the device and available for delivery; in detail, the average amount of vaccine powder emitted from the insufflator was 2.43 ± 0.07 mg, corresponding to 48.7 ± 1.37 μg of antigen. One week after the last immunization (total duration of the immunization protocol: 21 days) blood samples were collected by cardiac puncture and the resulting sera, obtained by blood centrifugation (20 min at 10000 x*g*) after 3 h at room temperature, were used to evaluate the immune responses in ELISA and neutralization assay

#### 2.2.12. ELISA

GST–L2 capture ELISA for anti-L2 antibody detection was carried out in 96-well microtiter plates pre-coated with glutathione-casein and subsequently blocked with casein buffer as described previously [38]. Individual immune sera were analyzed in duplicate by progressive (two-fold) serial dilutions starting from a 1:50 dilution, using a pool of pre-immune sera as control. Following serum addition and 1 h incubation at 37 °C, plates were washed three times and incubated with a HRP-conjugated goat anti-mouse secondary antibody (Sigma-Aldrich) previously diluted 1:5000 in PBS containing 0.3% *v/v* Tween-20 (PBS-T). Plates were incubated for 1 h at 37 °C, washed three times, and developed by adding the KPL ABTS Peroxidase Substrate [2,29-azino-bis(3-ethylbenz-thiazoline-6-sulfonic acid)] staining solution (SeraCare; 100 μL/well). Absorbance at 405 nm was measured after 30 min at 30 °C with a microplate reader (iMark™, Bio-Rad).

To evaluate protein antigen integrity, 96-well microtiter plates were coated with *Pf*Trx-HPV-L2 (5 μg/mL in PBS, 100 μL/well; o/n incubation at 4 °C) pre-exposed to different concentrations of ethanol (0, 1, 5, 10, 15, 20, 30, 50, 70%) and/or to spray-drying. After three washes with PBS-T, plates were blocked with 3% skim milk in PBS for 1 h at 37 °C. Serial dilutions of a monoclonal anti-L2 antibody [(K4L2(20–38), [39]] or an anti-*Pf*Trx mAb were then added, followed by three washes as above and incubation for 1 h at 37 °C with a HRP-conjugated goat anti-mouse secondary antibody (Sigma-Aldrich) diluted 1:5000 in PBS-T. After three additional washes, plates were developed by adding the KPL ABTS Peroxidase Substrate staining solution (100 μl/well) and read at 405 nm with a microplate reader (iMark™, Bio-Rad) after a 30 min incubation at 30 °C.

#### 2.2.13. Immunoglobulin isotyping

Immunoglobulin subclasses in sera from mice immunized with the different antigen formulations and modes of delivery were determined by ELISA using a mouse antibody isotyping kit (Pierce, Thermo Fisher Scientific) according to the manufacturer's instructions. A pool composed by equal volumes (100 μl each) of sera from the four best responding animals was employed as a test sample (50 μl fixed volume) that was added to ELISA strip-wells pre-coated with isotype-specific (IgG1, IgG2a, IgG2b, IgG3, IgM, IgA) anti-mouse heavy-chain capture antibodies and assayed in duplicate. Following incubation (1 h at RT under gentle shaking conditions) with HRP-conjugated, goat anti-mouse IgG + IgA + IgM detection antibodies and washing, the TMB substrate was added, incubated for 5–15 min, and colour development was read with a microplate reader at 405 nm.

#### 2.2.14. Neutralization assay

L2 pseudovirion-based neutralization assays (L2-PBNA) were performed as described previously [40,41]. Briefly, following MCF10A cells plating, propagation/lysis, extracellular matrix (ECM) deposition and washing, a pseudovirion solution, prepared in conditioned medium from CHO furin cells and supplemented with 5 μg/ml heparin (Sigma H-4784) in a total volume of 120 μL/well, was added to the ECM-coated wells. The virus-furin-heparin mixture was incubated overnight at 37 °C. The medium was then removed, and the wells were washed twice with PBS. The final wash was then replaced with the immune sera (100 μL/well of the same sera utilized for immunoglobulin isotype profiling) and serially diluted in pgsa-745 growth medium. The plate was incubated at 37 °C for 6 h to allow for antibody binding to the target L2 epitope, followed by addition of pgsa-745 reporter cells (50 μL 8 × $10^3$ cells/well). For all assays, sera were serially diluted in 3-fold dilution steps starting from an initial 1:50 dilution. The secreted Gaussia luciferase was determined with the coelenterazine substrate and Gaussia glow juice using a microplate luminometer (Victor3, PerkinElmer). Data were analyzed and 50% inhibitory concentrations (IC50) were determined using the GraphPad Prism software program.

#### 2.2.15. Statistical analysis

Unless otherwise indicated, all values are expressed as mean ± standard deviation. Statistical significance of differences was evaluated using two-tailed unpaired *t*-test with significance level set at a *p*-value ≤0.05. Statistical analysis was performed with Microsoft Excel version 16.18 (Microsoft Corporation) and the Prism 7 software version 7.0d (GraphPad Software).

## 3. Results and discussion

### 3.1. Pre-formulation of respirable particles loaded with the PfTrx-HPV-L2 antigen

Building upon previous work by Parlati et al. [23], we initially focused on the basic set-up of a DPI vaccine prototype using sodium stearate as a surfactant and a technological surrogate of the amphiphilic immune-adjuvant monophosphoryl lipid A (MPLA).

Spray-drying, which entails a temporary (in the order of milliseconds) exposure to fairly high temperatures (typically from 100 °C to 140 °C) and a rapid interface conversion, may be a rather harsh process, especially when applied to protein-based bioactive components that may undergo irreversible denaturation as well as oxidation. Based on the above considerations, in addition to the use of a thermostable protein antigen, we adopted a particle engineering approach, paying special attention to two key steps, namely: i) the use of a water-ethanol solution in order to dissolve the amphiphilic component of the final formulation, which, on one hand, would allow to reduce the inlet drying temperature but, on the other, may be detrimental to protein stability; and ii) the total amount of solute in the feed solution in order to obtain a suitable amount of powder at the end of the process. In fact, should the solute only be comprised of the antigen, extremely high protein concentrations would be required, with protein aggregation and subsequent precipitation. We thus resorted to the supplementation of the feed solution with a bulking agent. To this end, we conducted a pre-formulation study with mannitol, lactose and trehalose as potential excipients. As a result of this study, mannitol was selected as the best bulking agent in the tested experimental conditions due the superior production yields it afforded and the superior aerodynamic performance of the protein-containing powder (see Supplementary Table S2).

A further preliminary study indicated 70% *v*/v ethanol as the highest organic solvent content of the protein-containing (*Pf*Trx-HPV-L2: 1 mg/mL) hydro-alcoholic solution compatible with protein stability (see Supplementary Fig. S2). Thus, a 70:30 (*v/v*), water:ethanol solution was selected for the subsequent production of *Pf*Trx-HPV-L2 DPIs.

In parallel, the concentration of sodium stearate in the feed solution

**Table 1**
Manufacturing parameters and aerodynamic properties of antigen-lacking powders containing different amounts of sodium stearate.[a]

| Powder # | Sodium Stearate (% w/w) | pH of Feed Solution | Yield (%) | $D_{v,50}$ | EF (%) | RF (%) |
|---|---|---|---|---|---|---|
| 1 | – | 5.89 | 54.63 | 6.08 (0.74) | 87.51 (2.01) | 43.52 (4.01) |
| 2 | 0.33 | 5.88 | 31.53 | 18.58 (2.44) | 75.16 (5.17) | 8.02 (3.04) |
| 3 | 1.00 | 7.94 | 43.72 | 3.40 (0.73) | 89.89 (1.32) | 48.10 (9.39) |
| 4 | 2.00 | 8.14 | 59.46 | 26.35 (3.09) | 94.46 (2.69) | 13.59 (7.21) |

[a] Sodium stearate content (as percentage by weight of the solutes contained in the feed solution), production yield, pH of the feed solutions, median volume diameter ($D_{v,50}$), Emitted Fraction (EF, as percentage of the loaded amount) and Respirable Fraction (RF, as percentage of the loaded amount) of powders prepared with different amounts of sodium stearate. Mean values and standard deviations in parenthesis (n = 3).

(from 0.33 to 2.00% *w/w* of the solute) was investigated with respect to the particle size distribution (Table 1) and *in vitro* (fast screening) deposition of the resulting powders. The respirability *vs* sodium stearate concentration profile could be fitted to a quadratic equation with a maximum around 1% *w/w* sodium stearate, thus confirming previous data obtained in a similar experimental set-up [23].

Based on these pre-optimized experimental conditions, we then investigated the effect of an increased antigen content (*i.e.*, a *Pf*Trx-HPV-L2 starting concentration higher than 1 mg/ml and a correspondingly higher fractional protein content) on the physico-chemical properties of the resulting powders prepared with 1% sodium stearate. Three antigen concentrations, expressed as solute weights in the feed solution of 0.83, 1.33 and 2.00% *w/w*, were tested (Powders #3a, #3b and #3c). The particle size distribution and the aerodynamic behavior of the resulting powders are reported in Fig. 1.

At a 2.00% *w/w* antigen concentration (obtained by adding 1.5 mL of an 8 mg/mL protein solution to 100 mL of feed solution), a monomodal powder (span 1.28 ± 0.04, Fig. 1A) composed of highly respirable microparticles (RF = 70.9% ± 5.6) (Fig. 1B) was produced, with a spray-drying yield of approximately 65%. SDS-PAGE analysis (Fig. 2A) confirmed the presence of an apparently intact, dry-powder associated antigen, whose functional integrity (*i.e.*, the ability to be recognized by anti-HPV-L2 and anti-*Pf*Trx mAbs) was verified by ELISA (Fig. 2B).

### 3.2. Conversion of PfTrx-HPV-L2 into a prototype respiratory vaccine using GLA as a particle lubricant and a built-in immune-adjuvant

The presence of an immune-adjuvant is an essential prerequisite for subunit vaccine immunogenicity [1,2], including vaccines such as Gardasil and Cervarix that are made up by intrinsically highly immunogenic HPV-L1 pseudovirion components [25,26,28]. GLA is a synthetic derivative of MPLA, a low-toxicity lipopolysaccharide that is present as a biological adjuvant in various licensed vaccines, including Cervarix. GLA is an amphiphilic molecule that acts as an agonist of toll-like receptor 4 (TLR4) [42]. GLA itself [43] and its parent compound MPLA [20,27,44] have proved to be effective immune adjuvants when included in formulations for nasal and pulmonary administration. The amphiphilic nature of GLA prompted us to test its possible use as a sodium stearate replacement, capable of acting as both a coating agent enhancing particle flow, de-aggregation and ultimately respirability, as

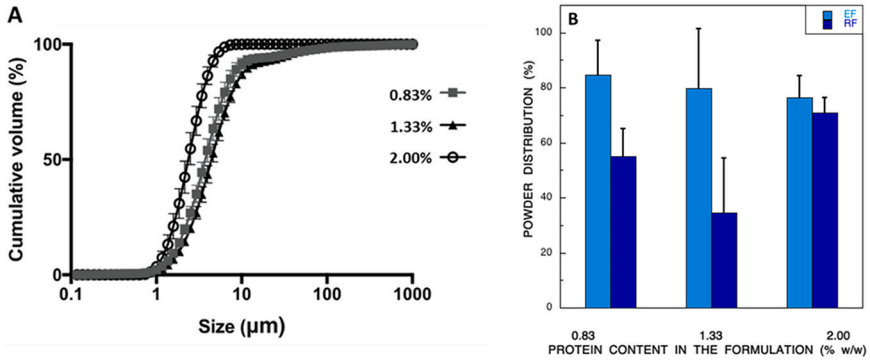


**Fig. 1.** (A) Particle cumulative undersize distribution evaluated by laser light diffraction of spray-dried powders 3a, #3b and #3c containing different amounts of the protein antigen: 0.83% *w/w* (*squares*), 1.33% *w/w* (*triangles*), 2.00% *w/w* (*empty circles*) (mean values and standard deviation bars are indicated; $n = 3$). (B) Emitted fraction (EF) and Respirable Fraction (RF) aerodynamic properties of the three powders, containing different amounts of the *Pf*Trx-HPV-L2 antigen as indicated. Mean and standard deviation values (n = 3) are indicated.

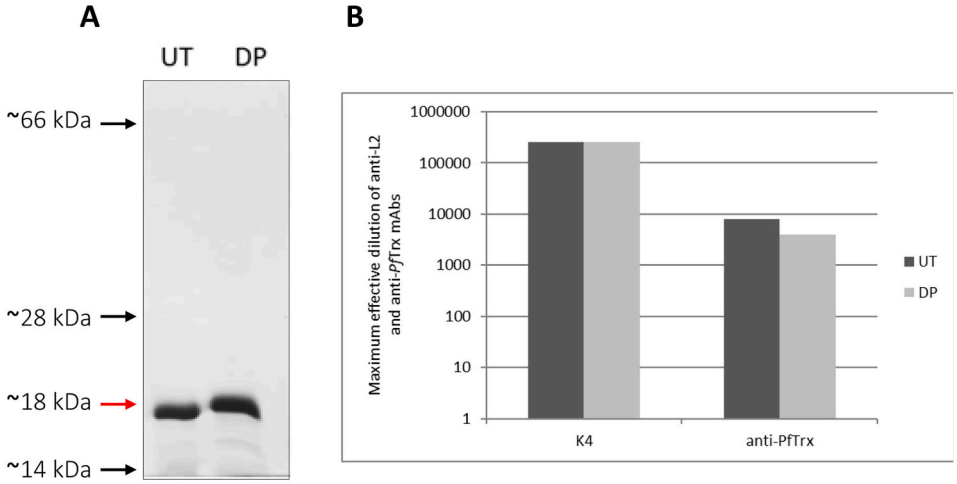


**Fig. 2.** (A) SDS-PAGE analysis of the untreated (UT) liquid-form and the dry-powder formulated (DP) *Pf*Trx-HPV-L2 antigen. The expected migration position of the *Pf*Trx-HPV-L2 protein is indicated by a *red arrow*; the migration positions of molecular mass markers are indicated by *black arrows*. (B) Comparative ELISA analysis of the immunoreactivity of the untreated (UT, *dark-grey*) and the dry-powder formulated (DP, *light-grey*) *Pf*Trx-HPV-L2 antigen. mAbs directed against the L2 epitope (K4) or the *Pyrococcus* thioredoxin scaffold (anti-*Pf*Trx) were used as primary antibodies, as indicated. The results are the average of two technical replicates, which differed by no more than 5% of the mean. (For interpretation of the references to colour in this figure legend, the reader is referred to the web version of this article.)

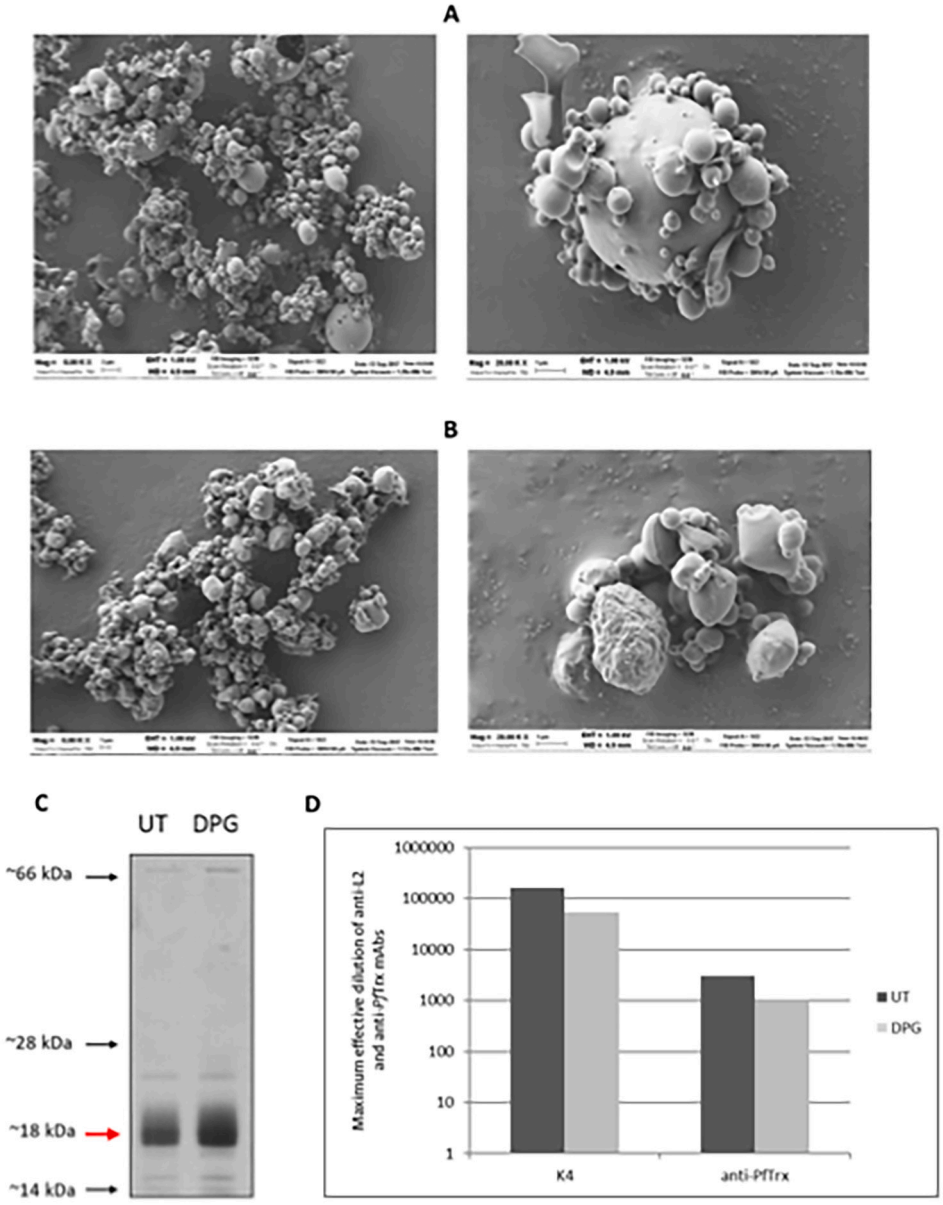


**Fig. 3.** SEM images of the GLA-containing powder #5 (1.33% *w/w* of *Pf*Trx-HPV-L2) (A) and powder #6 containing 2.00% *w/w* *Pf*Trx-HPV-L2 (B). Magnification 6.000× (*left-hand image*) and 20.000× (*right-hand image*). (C) SDS-PAGE analysis of the untreated liquid-form (UT) and the dry-powder-GLA formulated (DPG) *Pf*Trx-HPV-L2 antigen. The expected migration position of the *Pf*Trx-HPV-L2 protein is indicated by a *red arrow*; the migration positions of molecular mass markers are indicated by *black arrows*. (D) ELISA analysis of the untreated (UT, *dark-grey*) and the dry-powder-GLA formulated (DPG, *light-grey*) *Pf*Trx-HPV-L2 antigen. mAbs directed against the L2 epitope (K4) or the *Pyrococcus* thioredoxin scaffold (anti-*Pf*Trx) were used as primary antibodies for detection, as indicated. The results are the average of two technical replicates, which differed by no more than 5% of the mean. (For interpretation of the references to colour in this figure legend, the reader is referred to the web version of this article.)

well as a built-in immune-adjuvant.

We thus set out to incorporate GLA as a sodium stearate substitute in our *Pf*Trx-HPV-L2 microparticle formulation. As a first approximation, we estimated the amount of GLA that would be required to obtain a particle surface coating like that achieved with sodium stearate, starting from the assumption that a lower amount of a larger molecule is needed to cover the same surface. Based on the molecular weight ratio between sodium stearate (306.5 g/mol) and GLA (1763.5 g/mol), a 1% (*w/w*) fractional amount of sodium stearate corresponds to approximately 0.17% *w/w* GLA. With respect to the GLA concentration in the feed solution, this amount corresponds to 1.02 μg/ml, which is one order of magnitude lower than the reported CMC for MPLA [45]. Thus, also considering that the feed solution contained 30% *v/v* ethanol, we assumed that GLA was completely dissolved without micelle formation, which represents a key feature for the surfactant migration at the air/liquid interface of the droplets during the spray-drying process [23,46,47]. The adjuvant concentration we employed is significantly higher than that reported in the literature [20], thus allowing to assume that a relevant portion of the GLA distributed to the droplet air liquid interface during the drying process and, ultimately, on the microparticle surface.

A new powder, containing GLA as both an amphiphilic technological excipient with particle lubricant functionality and an immune adjuvant, was thus produced, starting from 4 and 12 mg/mL solutions of detoxified and filter-sterilized *Pf*Trx-HPV-L2 antigen dissolved in phosphate buffer. In this way, an antigen concentration in the final powder of 1.33% *w/w* (Powder #5) or 2% *w/w* (Powder #6) was obtained.

The resulting particles (production yields of 79 and 65%, respectively), which were mainly spherical in the case of 1.33% *Pf*Trx-HPV-L2 and more irregularly shaped for the higher (2.00% *w/w*) antigen concentration (Fig. 3A and B), featured a narrow mono-modal size distribution: for Powder #5 $D_{v,10} = 1.27 \pm 0.12$ μm, $D_{v,50}$ of $2.39 \pm 0.24$ μm, $D_{v,90} = 4.30 \pm 0.32$ μm, Span value = 1.27; for Powder #6 $D_{v,10} = 1.43 \pm 0.09$ μm, $D_{v,50} = 2.65 \pm 0.18$ μm, $D_{v,90} = 4.78 \pm 0.55$ μm, Span value = 1.26. The solution obtained upon particle solubilization in ultrapure water displayed a slightly basic pH (7.5 and 8.0 for Powder #5 and #6, respectively).

The lubricant functionality of GLA was compared to that of sodium stearate by evaluating the powder flow properties through the determination of the dynamic angle of repose according to Ph. Eur. 10th ed.

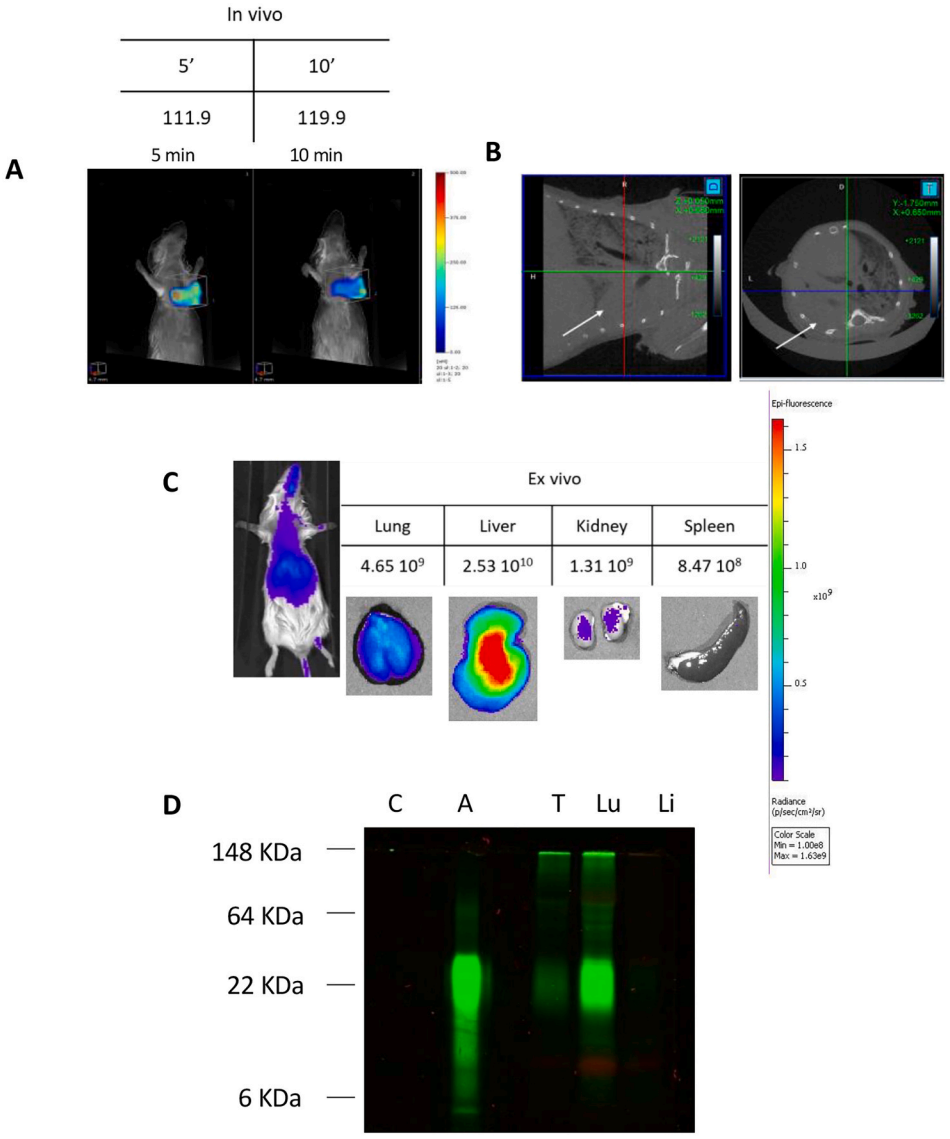


**Fig. 4.** Tissue distribution of the Alexa Fluor 750-labeled *Pf*Trx-HPV-L2 antigen delivered intratracheally in liquid form. Intratracheally administered, pre-dissolved Alexa-labeled vaccine powder visualized by FMT, 5 and 10 min after intratracheal delivery (A) and by Micro-CT (B) imaging (transversal and coronal views are shown in the left- and right-side images, respectively, where the arrows indicate the accumulation sites of the delivered liquid vaccine). *In vivo* (C, *left-side panel*) and *ex-vivo* multi-organ (C, *right-side panel*) IVIS imaging of the Alexa-labeled *Pf*Trx-HPV-L2 antigen 15 min after intratracheal administration. (D) SDS-PAGE fractionation and fluorescence-based visualization of trachea (T), lung (Lu) and liver (Li) tissue homogenates derived from a mouse, to which the pre-dissolved Alexa-labeled dry-powder vaccine was administered intratracheally; equivalent amounts (5 ng) of the unlabeled (C) and the Alexa-labeled (A) *Pf*Trx-HPV-L2 protein served as controls for this experiment. The results are from a representative experiment that was performed in parallel on two different animals.

This measurement was carried out on powders containing the same amount of antigen (1.33%). The GLA-containing powder had an angle of repose of 18.74 ± 1.48° indicative of excellent flow properties, at variance with the sodium stearate-containing powder which showed poor flowability (angle of repose = 46.6 ± 0.60°).

Aerosolization performance analysis, initially conducted with the RS01® device and a Fast Screening Impactor (FSI), yielded an Emitted Fraction (EF) of 86.0% ± 0.8 (Powder #5) and 81.3% ± 11.2 (Powder #6) and a Fine Particle Fraction (FPF) of 61.2% ± 8.6 (Powder #5) and 60.0% ± 2.0 (Powder #6).

To gain more detailed information on the aerodynamic particle size distribution of powder #6 (the one with the highest antigen content), aerodynamic performance was also assessed with an Andersen Cascade Impactor (ACI) through quantitative detection of mannitol in the impactor stages by a HPLC/RID method. Since the protein is embedded within GLA-coated, mannitol-containing particles, it was assumed that mannitol could be used as a reliable indicator of antigen emission from the device and its distribution within the different stages of the impactor. Mannitol emitted from RS01® was 12.5 ± 1.5 mg (EF = 64.2% ± 7.85), with a Fine Particle Mass (FPM) of approximately 9 ± 0.7 mg (RF = 72.3% ± 5.59) and a Median Mass Aerodynamic Diameter (MMAD) of 2.5 ± 0.1 μm.

A subset of powder #6-filled capsules was stored at room temperature under light-shielded conditions and re-tested 5 months after production. The mannitol EF was found to be approximately 10% higher compared to time zero; RF also increased (83.2% ± 12.1), although for both parameters the difference was not statistically significant with respect to the values recorded at time zero ($p > 0.5$); MMAD remained essentially the same. The presence of residual free water was excluded by Thermo-Gravimetric Analysis, which indicated a negligible water loss (<0.1%) upon heating (not shown), while Isothermal Dynamic Vapor Sorption measurements carried out at both 25 °C and 40 °C revealed the very low and completely reversible tendency of the powder to absorb humidity (see Supplementary Fig. S2). This can be ascribed both to the partial hydrophobic coating of the particle surface with GLA and to the fact that the spray-drying process yielded the β-form of mannitol (melting peak at 166 °C as revealed by DSC analysis; not shown), which represents the thermodynamically stable and non-hygroscopic crystal form of the bulking agent (*i.e.*, the most abundant component of the powder). As revealed by semi-quantitative SDS-PAGE analysis (Fig. 3C), the *Pf*Trx-HPV-L2 content of the GLA powder was in line with the amount expected based on the input concentration and fractional content of the protein. Importantly, the immunoreactivity of the solubilized spray-dried antigen (*i.e.*, the antigen retrieved from particles dissolved

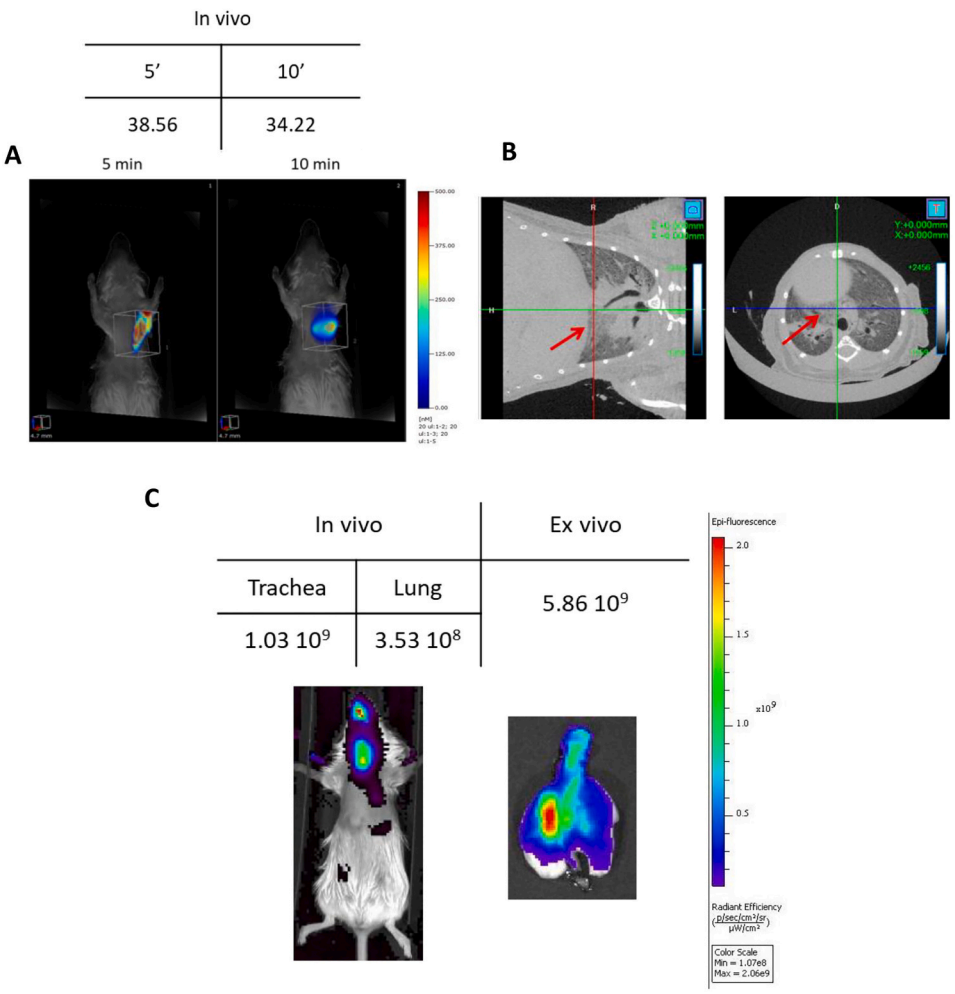


**Fig. 5.** Lung deposition of the intratracheally administered dry-powder vaccine. (A) *In vivo* total body FMT imaging of the Alexa Fluor 750-labeled *Pf*Trx-HPV-L2 antigen distribution at two different time-points (5 and 10 min) after administration of the vaccine powder. (B) Micro-CT imaging of antigen deposition into the lungs; transversal and coronal views are shown in the left- and right-side images, respectively, where the arrows indicate the vaccine powder deposition sites. (C) *In vivo* (*left panel*) and *ex-vivo* (*right panel*), IVIS analysis of Alexa Fluor 750-labeled *Pf*Trx-HPV-L2 accumulation in the respiratory tract, 15 min after intratracheal delivery of the dry-powder vaccine.

in aqueous buffer) revealed by ELISA was the same as that of the native antigen (Fig. 3D).

### 3.3. Lung deposition of the PfTrx-HPV-L2-[GLA] dry-powder vaccine administered intratracheally

To gain insight on the lung deposition capacity of the *Pf*Trx-HPV-L2-[GLA] vaccine (Powder #6) administered intratracheally, we set-up conditions for direct *in vivo* imaging of the antigen. To this end, we used the NIR–dye Alexa Fluor 750 to label the *Pf*Trx-HPV-L2 protein. The labeled protein was then incorporated into GLA-coated particles using the previously developed formulation procedure (spray-dry yield of 57.8% *w*/w). Prior to intratracheal delivery, the powder was subjected to an FSI aerodynamic evaluation, which yielded Emitted Fraction and Respirable Fraction values (87.2% ± 6.1 and 67.0% ± 4.8, respectively) superimposable to those obtained with the unlabeled protein-containing powder.

In a preliminary experiment aimed at setting-up mouse pulmonary administration conditions, the labeled dry-powder vaccine was dissolved in aqueous buffer prior to intratracheal delivery. As shown in Fig. 4A, the Alexa-labeled *Pf*Trx-HPV-L2 protein could be tracked in the lungs by FMT, with nearly the same fluorescence intensity at 5 and 10 min after delivery and a slightly preferential (but likely random) accumulation in the left lobe. This kind of distribution was confirmed by Micro-CT imaging, which allowed to visualize the fine anatomical details of the lung delivery site (Fig. 4B). As revealed by IVIS imaging, after 15 min the fluorescence signal became more diffuse and apparently spread to the liver and other sub-thoracic organs (Fig. 4C). Indeed, an intense fluorescence was detected not only in the lungs but also in the liver and other organs explanted after mouse sacrifice. To distinguish between protein-associated fluorescence and a spurious signal arising from protein degradation and release into the circulation of the Alexa dye (either free or associated to *Pf*Trx-HPV-L2 peptide fragments), trachea, lung and liver tissue homogenates from the same animal were examined by SDS-PAGE. As shown in Fig. 4D, a strong and a slightly weaker but well detectable fluorescence signal was found to be associated -in lung and trachea extracts, respectively- with a polypeptide displaying the same electrophoretic mobility as the authentic Alexa-labeled *Pf*Trx-HPV-L2 protein, whereas no fluorescence was detected in the case of the liver homogenate. This indicates that liver fluorescence was indeed associated to small-sized degradation products of the labeled *Pf*Trx-HPV-L2 protein, that ran out of the gel upon electrophoretic fractionation.

Next, a similar experiment was conducted with the *Pf*Trx-HPV-L2-[GLA] powder (2 mg, containing 12 μg of Alexa-labeled antigen), delivered intratracheally with the use of a modified dry powder insufflator device. As shown by the data presented in Fig. 5, also under these conditions, which closely mimic the actual set-up of mouse pulmonary vaccination, a fairly even antigen distribution within the respiratory tract, with a marked accumulation in the lungs, was revealed by *in-vivo* and *ex-vivo* analyses. Specifically, *in vivo* imaging by FMT revealed fluorescence signals of similar intensity in the lungs at both 5 and 10 min after administration (Fig. 5A). A more targeted localization to the chest region compared to the solubilized vaccine was revealed by IVIS

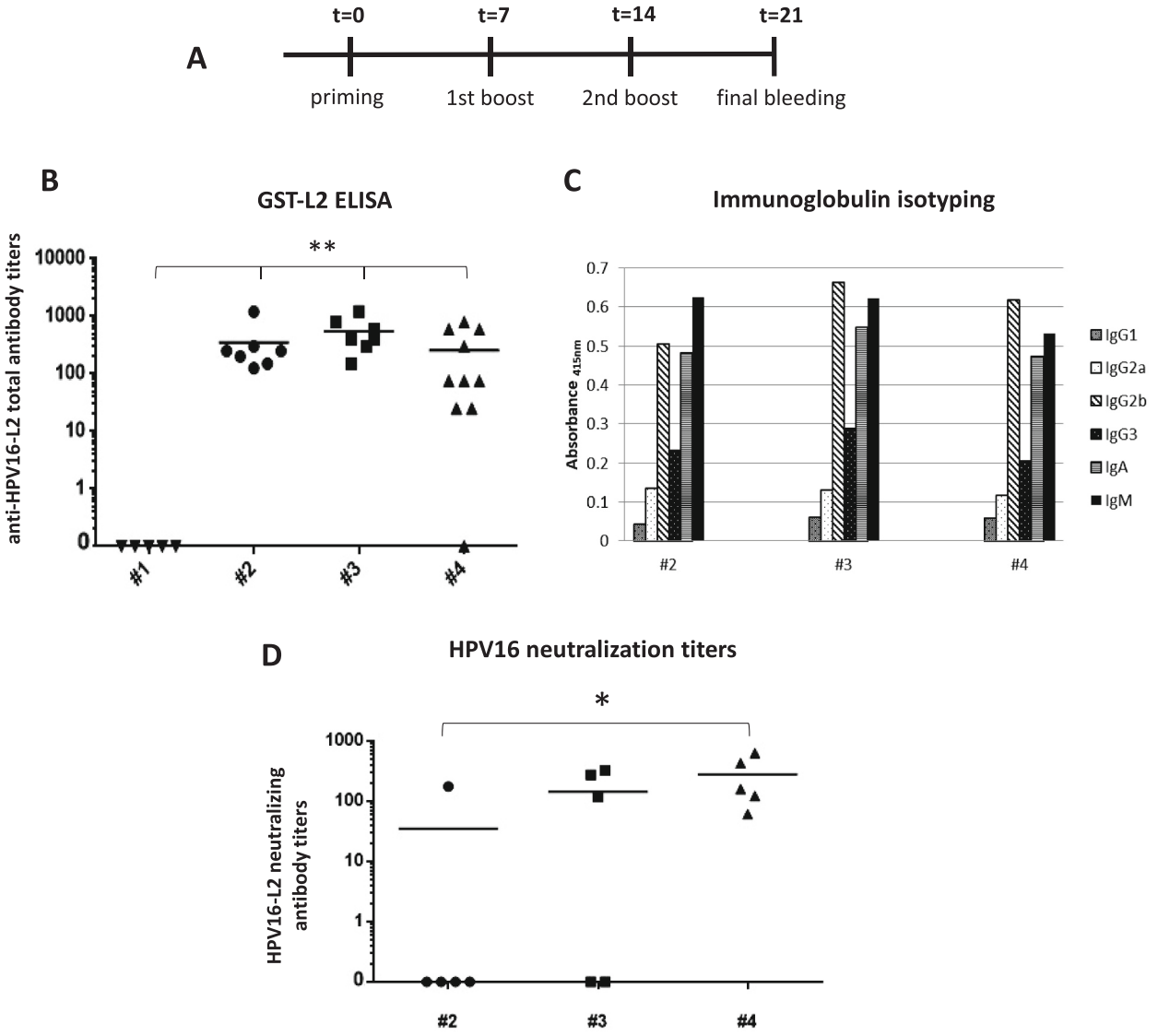


**Fig. 6.** Immunogenicity profiling. (A) Timeline of the short-term immunization experiment performed with the GLA-adjuvanted, *Pf*Trx-HPV-L2 DPI delivered intratracheally. (B) GST-L2 ELISA performed on sera from differently treated groups of mice, collected one week after the last immunization. The following treatments were applied to individual groups: #1, subcutaneous immunization with solubilized, GLA only containing powder with no antigen ('negative control'); #2, subcutaneously injected, liquid form, GLA + alum adjuvanted *Pf*Trx-HPV-L2 antigen; #3 subcutaneously injected *Pf*Trx-HPV-L2-[GLA] dry-powder vaccine solubilized in PBS immediately before administration; #4, *Pf*Trx-HPV-L2-[GLA] dry-powder vaccine administered intratracheally. Data represent anti-HPV-L2 total antibody titers measured in individual mice; the means of the titers for each group are indicated by horizontal lines (**$p \leq 0.01$). (C) Immunoglobulin isotyping of pooled sera from the mice groups (#2, #3 and #4) shown in panel B, except for the completely unresponsive, negative control group #1. (D) HPV16 neutralization titers determined by the L2-PBNA on a subset of five immune-sera/group (#2, #3 and #4) derived from the animals in each group that displayed the highest (top five) anti-HPV-L2 total antibody titers by GST-L2 ELISA (panel B). Data represent neutralizing antibody titers measured in individual mice; mean values of the titers for each group are indicated by horizontal lines (*$p \leq 0.05$).

imaging (*cf.* Fig. 5C with Fig. 4C). As shown in Fig. 5B, these results were confirmed by the more anatomically detailed visualization afforded by Micro-CT analysis.

Altogether, these data fully support the favorable aerodynamic properties and suitability for pulmonary administration of the *Pf*Trx-HPV-L2-[GLA] powder initially pointed out by the results of *in vitro* aerosolization analyses.

### 3.4. Preliminary evaluation of the immunogenicity of the pulmonary delivered PfTrx-HPV-L2-[GLA] dry-powder vaccine

A comparative, pulmonary *vs.* subcutaneous (s.c.) vaccination experiment was then set-up. This included the following treatment and control groups: group #1) s.c. injection of a solubilized, GLA-containing dry-powder lacking the antigen (negative control); group #2) s.c. injection of the liquid-form, alum+GLA-adjuvanted *Pf*Trx-HPV-L2 antigen; group #3) s.c. injection of the *Pf*Trx-HPV-L2-[GLA] dry-powder vaccine solubilized immediately before administration; group #4 the *Pf*Trx-HPV-L2-[GLA] dry-powder vaccine administered intratracheally.

To minimize the risk (and potential confounding effects) of bacterial infections associated to intratracheal delivery, we decided to use a short-schedule immunization protocol. This only involved two boost immunizations at a one-week interval, followed by final bleeding and immune sera collection after one more week (Fig. 6A). As shown by the ELISA data reported in Fig. 6B, very similar titers of total anti-L2 antibodies were detected in all groups, except for the antigen-lacking, negative

control. The fact that absolute titers (average value = 1:370) were significantly lower than those detected previously with the same antigen delivered subcutaneously [48] is likely explained by the short-term immunization protocol adopted in the present exploratory study (21 days with only two boost injections and final bleeding all one-week a part), compared to 72 days with three biweekly boost injections and a 1-month time-interval before sera collection [31,32,34].

We also determined the immunoglobulin isotype profile of the antibodies elicited by the different immunogens and modes of delivery. As shown in Fig. 6C, the immunoglobulin isotype distributions associated to the dry-powder and the liquid-form vaccines were quite similar. In both cases, the Th1-associated IgG2b and IgG3 isotypes were considerably (10-fold on average) more represented than the Th2-associated IgG1 isotype. This indicates a marked Th1 polarization of the immune response that was previously shown to be causally associated to the use of the GLA immune-adjuvant [42,43]. Also highly represented were the IgM and IgA immunoglobulins, with a slight prevalence of the latter isotype in the case of the dry-powder vaccine.

Despite the short immunization schedule employed for this exploratory experiment, we also determined the ability of the induced anti-L2 antibodies to neutralize HPV16 pseudovirions. To this end, we used the highly sensitive L2-based pseudovirion neutralization assay [41] to determine the presence of HPV16 neutralizing antibodies. As shown in Fig. 6D, the highest and most consistent titer (5 positives out of 5 tested serum samples) was detected in sera from mice immunized intratracheally with the dry-powder formulation (#4). Interestingly, a slightly lower and less consistent (3 positives out of 5 tested sera) but well detectable neutralizing response was also observed in mice subcutaneously immunized with the solubilized dry-powder vaccine (#3). Instead, a poor neutralizing response, with only one out of five tested sera capable of HPV16 pseudovirion neutralization, was observed for sera from mice immunized subcutaneously with the liquid vaccine formulation (#2). The latter result, which contrasts with the neutralization capacity previously documented for the liquid-form, Montanide ISA720-, Alum/MPLA- or AddaVAx-adjuvanted *Pf*Trx-HPV-L2 antigen administered subcutaneously using the standard 72 days immunization protocol [31,32,34,48], likely reflects the short-term immunization schedule utilized for this experiment and perhaps the lack of an adequate length of time for antibody affinity-maturation. Under these sub-optimal but highly stringent immunization conditions, the dry-powder formulated *Pf*Trx-HPV-L2-[GLA] vaccine administered intratracheally, thus appears to be superior to the liquid-form vaccine, at least with respect to the short-term induction of HPV16 neutralizing antibodies.

## 4. Conclusions

We have provided proof-of-concept validation of a novel particle engineering approach that allows to produce a highly respirable powder vaccine by exploiting GLA as a double-purpose component capable of acting as both a technological lubricant improving the aerodynamic properties of the powder and an immune adjuvant. Both features stem from the amphiphilic nature of the GLA molecule that partitions on the surface of the particles during spray-drying manufacturing.

We also exploited the thermostability of the *Pf*Trx-HPV-L2 antigen, which proved to be resistant to a fairly high ethanol concentration, for immediate drying of a mannitol-supplemented, antigen-containing solution. The resulting dry-powder vaccine, which was always handled under non-refrigerated conditions, did not change its physico-chemical or aerodynamic properties, and retained a fully intact antigen upon storage for five months at room temperature. Indirect evidence, such as powder vaccine immunogenicity and the marked Th1 polarization of the induced immune response, indicates that the relatively harsh conditions associated to spray-drying are also well tolerated by the GLA adjuvant.

An open question regards the applicability of the present approach to other, less sturdy antigens. However, preliminary results (not presented in this work) indicate that a good quality and immunogenic dry powder vaccine could also be obtained with a more complex and less thermostable antigen, in which *Pf*Trx-HPV-L2 is genetically fused to an oligomerization domain (OVX313) that converts the primary antigen into a heptameric nanoparticle form [49,50].

Pulmonary delivered powder vaccines have often been found to induce a superior immune response compared to their parenterally injected counterparts [7,21,22]. It is thus not so surprising that even in our preliminary, and largely sub-optimal immunization experiments, the intratracheally administered DPI vaccine outperformed the subcutaneously injected vaccine in the short-term induction of HPV16 neutralizing antibodies. The reasons for this apparent superiority remain to be clarified. They might be related to either the particulate nature of a dry-powder vaccine, which has previously been shown to enhance immunogenicity through a more efficient targeting of antigen presenting cells [7,21]; the closer physical association between the antigen and the GLA adjuvant inherent to the dry powder formulation; and/or to the large surface area and extensive vascularization of the lungs [18]. Interestingly, even the DPI vaccine solubilized right before subcutaneous injection, induced higher and more consistent neutralizing antibody titers than its liquid-form counterpart. Whether this is due to residual micro-particle aggregates that resisted complete dissolution or to a tighter association between the GLA adjuvant and the antigen that persists even after solubilization is presently not known. Also unknown, and worth of future, more detailed investigations is the ability of the *Pf*Trx-HPV-L2 vaccine (and its polytopic derivatives [49,50]) to induce a mucosal response in the lungs, but also in the genital tract. This, together with a more extensive characterization of the HPV neutralizing immune responses elicited by a longer-term immunization protocol, will also shed light on the cross-neutralization potential of the pulmonary delivered *Pf*Trx-HPV-L2 vaccine. Altogether, the data presented in this work represent a step forward toward the development of needle-free and easy to handle next-generation vaccines.

## Conflicts of interest

The authors declare no conflict of interest. A European patent application based on the results of this study has been filed (WO2019EP78277).

## Acknowledgments

GS was partly supported by a post-doc fellowship from the Inter-university Consortium for Biotechnology (CIB). This work, which also benefited from the resources made available within the COMP-HUB Initiative (Dept. Chemistry, Life Sciences and Environmental Sustainability), funded by the “Departments of Excellence” program of the Italian Ministry for Education, University and Research (MIUR, 2018–2022), was supported by a Regione Emilia Romagna POR-FESR grant (PG/2015/731196) to SO and RB.

## Appendix A. Supplementary data

Supplementary data to this article can be found online at https://doi.org/10.1016/j.jconrel.2021.11.002.

## References

[1] P. Piot, H.J. Larson, K.L. O'Brien, J. N'kengasong, E. Ng, S. Sow, et al., Immunization: vital progress, unfinished agenda, Nature 575 (2019) 119–129, https://doi.org/10.1038/s41586-019-1656-7.
[2] R. Rappuoli, M. Pizza, G. Del Giudice, E. De Gregorio, Vaccines, new opportunities for a new society, Proc. Natl. Acad. Sci. U. S. A. 111 (2014) 12288–12293, https://doi.org/10.1073/pnas.1402981111.
[3] R. Rappuoli, E. De Gregorio, G. Del Giudice, S. Phogat, S. Pecetta, M. Pizza, et al., Vaccinology in the post-COVID-19 era, Proc. Natl. Acad. Sci. U. S. A. 118 (2021), https://doi.org/10.1073/pnas.2020368118.

[4] C. Clendinen, Y. Zhang, R.N. Warburton, D.W. Light, Manufacturing costs of HPV vaccines for developing countries, Vaccine 34 (2016) 5984–5989, https://doi.org/10.1016/j.vaccine.2016.09.042.

[5] World Health Organization, The Controlled Temperature Chain (CTC): Frequently Asked Questions. https://www.who.int/immunization/programmes_systems/supply_chain/resources/Controlled-Temperature-Chain-FAQ.pdf?ua=1, 2021 (accessed 2021, January 31st).

[6] Y. Nir, A. Paz, E. Sabo, I. Potasman, Fear of injections in young adults: prevalence and associations, Am. J. Trop Med. Hyg. 68 (2003) 341–344.

[7] T. Sou, E.N. Meeusen, M. de Veer, D.A.V. Morton, L.M. Kaminskas, M.P. McIntosh, New developments in dry powder pulmonary vaccine delivery, Trends Biotechnol. 29 (2011) 191–198, https://doi.org/10.1016/j.tibtech.2010.12.009.

[8] D.A. LeClair, E.D. Cranston, Z. Xing, M.R. Thompson, Optimization of spray drying conditions for yield, particle size and biological activity of thermally stable viral vectors, Pharm. Res. 33 (2016) 2763–2776, https://doi.org/10.1007/s11095-016-2003-4.

[9] S. Ohtake, R.A. Martin, L. Yee, D. Chen, D.D. Kristensen, D. Lechuga-Ballesteros, et al., Heat-stable measles vaccine produced by spray drying, Vaccine 28 (2010) 1275–1284, https://doi.org/10.1016/j.vaccine.2009.11.024.

[10] T. Sou, D.A.V. Morton, M. Williamson, E.N. Meeusen, L.M. Kaminskas, M. P. McIntosh, Spray-dried influenza antigen with trehalose and leucine produces an aerosolizable powder vaccine formulation that induces strong systemic and mucosal immunity after pulmonary administration, J. Aerosol Med. Pulm. Drug Deliv. 28 (2015) 361–371, https://doi.org/10.1089/jamp.2014.1176.

[11] D.A. LeClair, E.D. Cranston, Z. Xing, M.R. Thompson, Evaluation of excipients for enhanced thermal stabilization of a human type 5 adenoviral vector through spray drying, Int. J. Pharm. 506 (2016) 289–301, https://doi.org/10.1016/j.ijpharm.2016.04.067.

[12] S. Afkhami, D.A. LeClair, S. Haddadi, R. Lai, S.P. Toniolo, H.C. Ertl, et al., Spray dried human and chimpanzee adenoviral-vectored vaccines are thermally stable and immunogenic in vivo, Vaccine 35 (2017) 2916–2924, https://doi.org/10.1016/j.vaccine.2017.04.026.

[13] F. Emami, A. Vatanara, E.J. Park, D.H. Na, Drying technologies for the stability and bioavailability of biopharmaceuticals, Pharmaceutics 10 (2018) 131, https://doi.org/10.3390/pharmaceutics10030131.

[14] M.L. Levy, W. Carroll, J.L. Izquierdo Alonso, C. Keller, F. Lavorini, L. Lehtimäki, Understanding dry powder inhalers: key technical and patient preference attributes, Adv. Ther. 36 (2019) 2547–2557, https://doi.org/10.1007/s12325-019-01066-6.

[15] M.L. Cohn, C.L. Davis, G. Middlebrook, Airborne immunization against tuberculosis, Science 128 (1958) 1282–1283, https://doi.org/10.1126/science.128.3334.1282.

[16] R.H. Waldman, J.J. Mann, P.A. Small, Immunization against influenza. Prevention of illness in man by aerosolized inactivated vaccine, Jama 207 (1969) 520–524, https://doi.org/10.1001/jama.207.3.520.

[17] J. Tomar, P.A. Born, H.W. Frijlink, W.L.J. Hinrichs, Dry influenza vaccines: towards a stable, effective and convenient alternative to conventional parenteral influenza vaccination, Exp. Rev. Vacc. 15 (2016) 1431–1447, https://doi.org/10.1080/14760584.2016.1182869.

[18] N. Marasini, L.M. Kaminskas, Subunit-based mucosal vaccine delivery systems for pulmonary delivery - are they feasible? Drug Dev. Ind. Pharm. 45 (2019) 882–894, https://doi.org/10.1080/03639045.2019.1583758.

[19] T.T. Mutukuri, N.E. Wilson, L.S. Taylor, E.M. Topp, Q.T. Zhou, Effects of drying method and excipient on the structure and physical stability of protein solids: Freeze drying vs. spray freeze drying, Int. J. Pharm. 594 (2021) 120169, https://doi.org/10.1016/j.ijpharm.2020.120169.

[20] H.P. Patil, S. Murugappan, W. ter Veer, T. Meijerhof, A. de Haan, H.W. Frijlink, et al., Evaluation of monophosphoryl lipid a as adjuvant for pulmonary delivered influenza vaccine, J. Control. Release 174 (2014) 51–62, https://doi.org/10.1016/j.jconrel.2013.11.013.

[21] C. Thomas, V. Gupta, F. Ahsan, Particle size influences the immune response produced by hepatitis B vaccine formulated in inhalable particles, Pharm. Res. 27 (2010) 905–919, https://doi.org/10.1007/s11095-010-0094-x.

[22] J.-P. Amorij, V. Saluja, A.H. Petersen, W.L.J. Hinrichs, A. Huckriede, H.W. Frijlink, Pulmonary delivery of an inulin-stabilized influenza subunit vaccine prepared by spray-freeze drying induces systemic, mucosal humoral as well as cell-mediated immune responses in BALB/c mice, Vaccine 25 (2007) 8707–8717, https://doi.org/10.1016/j.vaccine.2007.10.035.

[23] C. Parlati, P. Colombo, F. Buttini, P.M. Young, H. Adi, A.J. Ammit, et al., Pulmonary spray dried powders of tobramycin containing sodium stearate to improve aerosolization efficiency, Pharm. Res. 26 (2009) 1084–1092, https://doi.org/10.1007/s11095-009-9825-2.

[24] F. Martinelli, A.G. Balducci, A. Kumar, F. Sonvico, B. Forbes, R. Bettini, et al., Engineered sodium hyaluronate respirable dry powders for pulmonary drug delivery, Int. J. Pharm. 517 (2017) 286–295, https://doi.org/10.1016/j.ijpharm.2016.12.002.

[25] J.T. Schiller, M. Müller, Next generation prophylactic human papillomavirus vaccines, Lancet Oncol. 16 (2015) e217–e225, https://doi.org/10.1016/S1470-2045(14)71179-9.

[26] Storage and Handling of GARDASIL®9, Human Papillomavirus 9-valent Vaccine, Recombinant. https://www.merckvaccines.com/gardasil9/storage-handling/ (accessed 2021, January 31st).

[27] V. Revaz, R. Zurbriggen, C. Moser, J.T. Schiller, F. Ponci, M. Bobst, et al., Humoral and cellular immune responses to airway immunization of mice with human papillomavirus type 16 virus-like particles and mucosal adjuvants, Antivir. Res. 76 (2007) 75–85, https://doi.org/10.1016/j.antiviral.2007.05.005.

[28] N.K. Kunda, J. Peabody, L. Zhai, D.N. Price, B. Chackerian, E. Tumban, et al., Evaluation of the thermal stability and the protective efficacy of spray-dried HPV vaccine, Gardasil® 9, Hum. Vaccin Immunother. 15 (2019) 1995–2002, https://doi.org/10.1080/21645515.2019.1593727.

[29] S. Saboo, E. Tumban, J. Peabody, D. Wafula, D.S. Peabody, B. Chackerian, et al., Optimized formulation of a thermostable spray-dried virus-like particle vaccine against human papillomavirus, Mol. Pharm. 13 (2016) 1646–1655, https://doi.org/10.1021/acs.molpharmaceut.6b00072.

[30] R.L. Garcea, N.M. Meinerz, M. Dong, H. Funke, S. Ghazvini, T.W. Randolph, Single-administration, thermostable human papillomavirus vaccines prepared with atomic layer deposition technology, NPJ Vacc. 5 (2020) 45–48, https://doi.org/10.1038/s41541-020-0195-4.

[31] E. Canali, A. Bolchi, G. Spagnoli, H. Seitz, I. Rubio, T.A. Pertinhez, et al., A high-performance thioredoxin-based scaffold for peptide immunogen construction: proof-of-concept testing with a human papillomavirus epitope, Sci. Rep. 4 (2014) 4729, https://doi.org/10.1038/srep04729.

[32] H. Seitz, L. Ribeiro-Müller, E. Canali, A. Bolchi, M. Tommasino, S. Ottonello, et al., Robust in vitro and in vivo neutralization against multiple high-risk HPV types induced by a thermostable thioredoxin-L2 vaccine, Cancer Prev. Res. (Phila.) 8 (2015) 932–941, https://doi.org/10.1158/1940-6207.CAPR-15-0164.

[33] B. Huber, J.W. Wang, R.B.S. Roden, R. Kirnbauer, RG1-VLP and other L2-based, broad-spectrum HPV vaccine candidates, J. Clin. Med. 10 (2021) 1044, https://doi.org/10.3390/jcm10051044.

[34] I. Rubio, A. Bolchi, N. Moretto, E. Canali, L. Gissmann, M. Tommasino, et al., Potent anti-HPV immune responses induced by tandem repeats of the HPV16 L2 (20 – 38) peptide displayed on bacterial thioredoxin, Vaccine 27 (2009) 1949–1956, https://doi.org/10.1016/j.vaccine.2009.01.102.

[35] S. Liu, R. Tobias, S. McClure, G. Styba, Q. Shi, G. Jackowski, Removal of endotoxin from recombinant protein preparations, Clin. Biochem. 30 (1997) 455–463, https://doi.org/10.1016/s0009-9120(97)00049-0.

[36] E. Gasteiger, C. Hoogland, A. Gattiker, S. Duvaud, M.R. Wilkins, R.D. Appel, Protein identification and analysis tools on the ExPASy server, in: J.M. Walker (Ed.), The Proteomics Protocols Handbook, 2021, pp. 571–607, n.d.

[37] F. Ruscitti, F. Ravanetti, V. Bertani, L. Ragionieri, L. Mecozzi, N. Sverzellati, et al., Quantification of lung fibrosis in IPF-like mouse model and pharmacological response to treatment by micro-computed tomography, Front. Pharmacol. 11 (2020) 1117, https://doi.org/10.3389/fphar.2020.01117.

[38] P. Sehr, K. Zumbach, M. Pawlita, A generic capture ELISA for recombinant proteins fused to glutathione S-transferase: validation for HPV serology, J. Immunol. Methods 253 (2001) 153–162, https://doi.org/10.1016/s0022-1759(01)00376-3.

[39] I. Rubio, H. Seitz, E. Canali, P. Sehr, A. Bolchi, M. Tommasino, et al., The N-terminal region of the human papillomavirus L2 protein contains overlapping binding sites for neutralizing, cross-neutralizing and non-neutralizing antibodies, Virology 409 (2011) 348–359, https://doi.org/10.1016/j.virol.2010.10.017.

[40] H. Seitz, T. Dantheny, F. Burkart, S. Ottonello, M. Müller, Influence of oxidation and multimerization on the immunogenicity of a thioredoxin-l2 prophylactic papillomavirus vaccine, Clin. Vaccine Immunol. 20 (2013) 1061–1069, https://doi.org/10.1128/CVI.00195-13.

[41] P.M. Day, Y.Y.S. Pang, R.C. Kines, C.D. Thompson, D.R. Lowy, J.T. Schiller, A human papillomavirus (HPV) in vitro neutralization assay that recapitulates the in vitro process of infection provides a sensitive measure of HPV L2 infection-inhibiting antibodies, Clin. Vaccine Immunol. 19 (2012) 1075–1082, https://doi.org/10.1128/CVI.00139-12.

[42] R.N. Coler, S. Bertholet, M. Moutaftsi, J.A. Guderian, H.P. Windish, S.L. Baldwin, et al., Development and characterization of synthetic glucopyranosyl lipid adjuvant system as a vaccine adjuvant, PLoS One 6 (2011), e16333, https://doi.org/10.1371/journal.pone.0016333.

[43] M.A. Arias, G.A. Van Roey, J.S. Tregoning, M. Moutaftsi, R.N. Coler, H.P. Windish, et al., Glucopyranosyl lipid adjuvant (GLA), a synthetic TLR4 agonist, promotes potent systemic and mucosal responses to intranasal immunization with HIVgp140, PLoS One 7 (2012), e41144, https://doi.org/10.1371/journal.pone.0041144.

[44] N.K. Childers, K.L. Miller, G. Tong, J.C. Llarena, T. Greenway, J.T. Ulrich, et al., Adjuvant activity of monophosphoryl lipid a for nasal and oral immunization with soluble or liposome-associated antigen, Infect. Immun. 68 (2000) 5509–5516, https://doi.org/10.1128/iai.68.10.5509-5516.2000.

[45] N.C. Santos, A.C. Silva, M.A.R.B. Castanho, J. Martins-Silva, C. Saldanha, Evaluation of lipopolysaccharide aggregation by light scattering spectroscopy, Chembiochem 4 (2003) 96–100, https://doi.org/10.1002/cbic.200390020.

[46] S. Belotti, A. Rossi, P. Colombo, R. Bettini, D. Rekkas, S. Politis, et al., Spray-dried amikacin sulphate powder for inhalation in cystic fibrosis patients: the role of ethanol in particle formation, Eur. J. Pharm. Biopharm. 93 (2015) 165–172, https://doi.org/10.1016/j.ejpb.2015.03.023.

[47] R. Vehring, Pharmaceutical particle engineering via spray drying, Pharm. Res. 25 (2008) 999–1022, https://doi.org/10.1007/s11095-007-9475-1.

[48] G. Spagnoli, A. Bolchi, D. Cavazzini, S. Pouyanfard, M. Müller, S. Ottonello, Secretory production of designed multipeptides displayed on a thermostable bacterial thioredoxin scaffold in Pichia pastoris, Protein Expr. Purif. 129 (2017) 150–157, https://doi.org/10.1016/j.pep.2016.04.012.

[49] G. Spagnoli, S. Pouyanfard, D. Cavazzini, E. Canali, S. Maggi, M. Tommasino, et al., Broadly neutralizing antiviral responses induced by a single-molecule HPV vaccine based on thermostable thioredoxin-L2 multiepitope nanoparticles, Sci. Rep. 7 (2017) 18000, https://doi.org/10.1038/s41598-017-18177-1.

[50] S. Pouyanfard, G. Spagnoli, L. Bulli, K. Balz, F. Yang, C. Odenwald, et al., Minor capsid protein L2 polytope induces broad protection against oncogenic and mucosal human papillomaviruses, J. Virol. 92 (2018), https://doi.org/10.1128/JVI.01930-17.